

 Open access • Journal Article • DOI:10.1142/S0218202513400113

Coupling traffic flow networks to pedestrian motion — [Source link](#)

Raul Borsche, Axel Klar, Sebastian Kühn, Anne Meurer

Institutions: Kaiserslautern University of Technology

Published on: 01 Feb 2014 - Mathematical Models and Methods in Applied Sciences (World Scientific Publishing Company)

Topics: Microscopic traffic flow model, Traffic wave, Fundamental diagram of traffic flow and Three-phase traffic theory

Related papers:

- [From the Microscale to Collective Crowd Dynamics](#)
- [A continuum theory for the flow of pedestrians](#)
- [The flow of human crowds](#)
- [A Hierarchy of Heuristic-Based Models of Crowd Dynamics](#)
- [Social Force Model for Pedestrian Dynamics](#)

Share this paper:    

View more about this paper here: <https://typeset.io/papers/coupling-traffic-flow-networks-to-pedestrian-motion-4intozyjdr>

COUPLING TRAFFIC FLOW NETWORKS TO PEDESTRIAN MOTION

R. Borsche (borsche@mathematik.uni-kl.de)

A. Klar (klar@mathematik.uni-kl.de)

S. Kühn (kuehn@mathematik.uni-kl.de)

A. Meurer (meurer@mathematik.uni-kl.de)

*Department of Mathematics, University of Kaiserslautern,
P.O.Box 3049, 67653 Kaiserslautern, Germany.*

In the present paper scalar macroscopic models for traffic and pedestrian flows are coupled and the resulting system is investigated numerically. For the traffic flow the classical Lighthill-Whitham model on a network of roads and for the pedestrian flow the Hughes model are used. These models are coupled via terms in the fundamental diagrams modeling an influence of the traffic and pedestrian flow on the maximal velocities of the corresponding models. Several physical situations, where pedestrians and cars interact, are investigated.

Keywords: traffic, pedestrians, networks, coupling

2010 AMS Subject Classification:

1. Introduction

In recent years a large number of models for traffic and pedestrian flow have appeared on different levels of description. For a recent review on traffic and pedestrian flow models see [5].

On the microscopic level, models which are based on Newton's equations have been developed for traffic flow among many others in [32, 7, 24] and for pedestrian flow in [22, 21, 4]. See [5] for further references in both cases. Traffic and pedestrian flow equations on the mesoscopic or kinetic level can be found for example in [35, 33, 29, 20, 14]. Macroscopic traffic and pedestrian flow equations involving equations for density and mean velocity of the flow are derived in [40, 3, 13, 2, 17, 16, 19] and [20, 6]. The classical macroscopic traffic flow model based on scalar continuity equations is described in [37]. Traffic models on networks for this equation can be found among many others in [25, 26, 9, 23, 18]. In [27, 28, 15, 10] pedestrian traffic modeling with scalar conservation laws based on the solution of the eikonal equation have been presented and investigated, see again [5] for further developments and historical comments. Additionally, in [5, 6], a variety of other macroscopic models are discussed.

The purpose of the present paper is to develop and investigate a model coupling

pedestrian and traffic flow simulations and describing the interaction of the two types of flows. We restrict ourselves to coupling scalar macroscopic models.

Traffic flow is considered on a network using a Lighthill-Whitham equation and coupling conditions at the nodes of the network as discussed in [26, 9]. Pedestrian flow is described using the model in [27, 28], where a nonlocal term including a global knowledge of the physical setting described by the eikonal equation is included into the continuity equation.

Both models are coupled together via their flux functions. The state of the vehicular traffic on the one hand influences the pedestrian velocity. On the other hand the fundamental diagram for the traffic is influenced by the pedestrian density. The numerical methods are based on a first order approach and use a straightforward splitting method to couple the two equations.

The paper is organized in the following way: in section 2 the macroscopic traffic flow model on a network and the pedestrian model are presented. Section 3 contains the coupling conditions for the two models. Section 4 describes the numerical methods and shows numerical results for several different physical situations including crosswalks and more complicated network situations.

2. The traffic network model and the optimal path pedestrian model

2.1. The traffic model

We consider the scalar Lighthill-Whitham traffic flow model. The car density $\rho = \rho(x, t)$, $x \in \mathbb{R}$, $t \in \mathbb{R}^+$, $\rho : \mathbb{R} \times \mathbb{R}^+ \rightarrow \mathbb{R}^+$ is governed by the equation

$$\partial_t \rho + \partial_x (f(\rho)) = 0 \quad (2.1)$$

with $f(\rho) = \rho V(\rho)$ and $f : (0, \rho_m) \rightarrow \mathbb{R}^+$. Here, f denotes the traffic flux and V is the velocity function for traffic flow with the maximal velocity $V(0) = V_m$, $V(\rho_m) = 0$. V is chosen such that $(\rho V)' = V + \rho V'$ is zero for a value $\sigma \in (0, \rho_m)$, positive for smaller values of ρ and negative for larger ones. The simplest example is given by the function

$$V(\rho) = V_m(1 - \rho/\rho_m). \quad (2.2)$$

The traffic network is described in the usual way: a finite number of roads are represented by intervals $[a_i, b_i]$, where a_i and b_i are the vertices of road e_i . We solve $\partial_t \rho_i + \partial_x f_i(\rho_i) = 0$ on every edge $e_i = (a_i, b_i)$. To find the junction value $\bar{\rho}_i$ which is derived from $\hat{\rho}_i = \rho_i((b_i)_-)$ for ingoing edges and $\hat{\rho}_i = \rho_i((a_i)_+)$ for outgoing edges we use the coupling conditions as defined in [9]. The first condition is given by the conservation of fluxes at the junctions

$$\sum_{i=1}^n f(\bar{\rho}_i) = \sum_{j=n+1}^{n+m} f(\bar{\rho}_j),$$

where ρ_i , $i = 1, \dots, n$ are the car densities on incoming roads while ρ_j , $j = n + 1, \dots, n + m$ are the car densities on outgoing roads. However, these conditions are not sufficient to obtain a unique solution on the network problem.

To state further coupling conditions we introduce the following notations as defined in [9]. We denote the distribution rates at the junctions by

$$A := \{\alpha_{ji}\}_{j=n+1, \dots, n+m; i=1, \dots, n} \in \mathbb{R}^{m \times n},$$

such that

$$0 \leq \alpha_{ji} \leq 1, \quad \sum_{j=n+1}^{n+m} \alpha_{ji} = 1,$$

where α_{ji} denotes the distribution rate from edge e_i to edge e_j . Moreover, we define the sets

$$\Omega_i := \begin{cases} [0, f(\hat{\rho}_i)], & \text{if } 0 \leq \hat{\rho}_i \leq \sigma \\ [0, f(\sigma)], & \text{if } \sigma \leq \hat{\rho}_i \leq \rho_{max} \end{cases} \quad i = 1, \dots, n, \quad (2.3)$$

$$\Omega_j := \begin{cases} [0, f(\sigma)], & \text{if } 0 \leq \hat{\rho}_j \leq \sigma \\ [0, f(\hat{\rho}_j)], & \text{if } \sigma \leq \hat{\rho}_j \leq \rho_{max} \end{cases} \quad j = n + 1, \dots, n + m, \quad (2.4)$$

and define the maximal possible flux on every incoming road as

$$c_i = \max_{c \in \Omega_i} c, \quad i = 1, \dots, n,$$

and c_j , the maximal possible flux on every outgoing road, respectively. We restrict from now on to junctions with three roads and use the so called NON-FIFO model [26, 23] for three roads. The coupling conditions on $\bar{\rho}_i$ are stated first as conditions on the fluxes γ_i on road e_i . In case of one ingoing road e_i with $i = 1$ and two outgoing roads e_j with $j = 2, 3$ we use

$$\gamma_2 := \min(\alpha_{21}c_1, c_2),$$

$$\gamma_3 := \min(\alpha_{31}c_1, c_3),$$

$$\gamma_1 := \gamma_2 + \gamma_3.$$

In the situation of two ingoing roads e_i with $i = 1, 2$ and one outgoing road e_3 we have to consider two possible cases:

- (1) $c_1 + c_2 > c_3$, i.e. the outgoing road has not enough capacity for the whole incoming flow. Then,

$$\gamma_1 := \min\left(c_1, \max\left(c_3 - c_2, \frac{c_3}{2}\right)\right),$$

$$\gamma_2 := \min\left(c_2, \max\left(c_3 - c_1, \frac{c_3}{2}\right)\right),$$

$$\gamma_3 := \gamma_1 + \gamma_2.$$

- (2) $c_1 + c_2 < c_3$, i.e the outgoing edge has enough capacity for the whole incoming flow. Then,

$$\begin{aligned}\gamma_1 &:= c_1, \\ \gamma_2 &:= c_2, \\ \gamma_3 &:= \gamma_1 + \gamma_2.\end{aligned}$$

To find the corresponding densities $\bar{\rho}_i$ we define as in [9] a function $\tau : [0, \rho_{max}] \rightarrow [0, \rho_{max}]$, $\tau(\sigma) = \sigma$, as a map satisfying the following condition

$$\tau(\rho) \neq \rho, \quad f(\tau(\rho)) = f(\rho),$$

for each $\rho \neq \sigma$. Then, for $i \in \{1, \dots, n\}$, let $\bar{\rho}_i \in [0, \rho_{max}]$ such that

$$f(\bar{\rho}_i) = \gamma_i, \quad \bar{\rho}_i \in \begin{cases} \{\hat{\rho}_i\} \cup (\tau(\hat{\rho}_i), \rho_{max}] & \text{if } 0 \leq \hat{\rho}_i \leq \sigma, \\ [\sigma, \rho_{max}] & \text{if } \sigma \leq \hat{\rho}_i \leq \rho_{max}. \end{cases}$$

For $j \in \{n+1, \dots, n+m\}$, let $\bar{\rho}_j \in [0, \rho_{max}]$ be such that

$$f(\bar{\rho}_j) = \gamma_j, \quad \bar{\rho}_j \in \begin{cases} [0, \sigma] & \text{if } 0 \leq \hat{\rho}_j \leq \sigma, \\ \{\hat{\rho}_j\} \cup [0, \tau(\hat{\rho}_j)) & \text{if } \sigma \leq \hat{\rho}_j \leq \rho_{max}. \end{cases}$$

With the above definitions we are able to find a unique solution to the Lighthill-Whitham equations on a network [9].

2.2. Pedestrian model

We consider the pedestrian model of Hughes [27], where the crowd density is denoted as $\xi = \xi(\mathbf{x})$, $\mathbf{x} \in \mathbb{R}^2$, with $\xi : \mathbb{R}^2 \rightarrow \mathbb{R}^+$, and the flux function as $\mathbf{F} : (0, \xi_m) \rightarrow \mathbb{R}^2$. Then the equation is given by

$$\partial_t \xi + \nabla_{\mathbf{x}} \mathbf{F}(\xi) = 0$$

with

$$\mathbf{F} = \xi U \mathbf{Z}, \tag{2.5}$$

where $U \in \mathbb{R}$ describes the crowd velocity and $\mathbf{Z} \in \mathbb{R}^2$, with $\|\mathbf{Z}\| = 1$ indicates the desired walking direction. The classical choice for the velocity function is the same as in the traffic case

$$U(\xi) = U_m (1 - \xi/\xi_m). \tag{2.6}$$

Moreover, the walking direction is given by

$$\mathbf{Z} = \frac{\nabla \Phi}{\|\nabla \Phi\|}$$

where Φ , with $\Phi : \mathbb{R}^2 \rightarrow \mathbb{R}$ is determined by solving the eikonal equation

$$U(\xi(\mathbf{x})) \|\nabla \Phi(\mathbf{x})\| = 1. \tag{2.7}$$

Altogether this gives the system of equations

$$\partial_t \xi + \nabla_{\mathbf{x}} \left(\xi U(\xi) \frac{\nabla \Phi(\mathbf{x})}{\|\nabla \Phi(\mathbf{x})\|} \right) = 0. \quad (2.8)$$

combined with (2.7).

Boundary conditions for Φ are chosen as $\Phi = 0$ on $\partial\Omega_D$, where $\partial\Omega_D$ denotes the pedestrians aim and with $\Phi = \infty$ otherwise.

3. The coupling

For the construction of a suitable coupling, we can re-use some ideas of the design of the separate models. We start with the description of the influence of the pedestrians on the flow of cars on the roads.

3.1. Pedestrian to traffic

A road is an object with spatial extension in two space dimensions, but the car traffic is modeled by 1D equations. In order to match both models, we average the density of the pedestrians on the road $\tilde{\xi}(x)$, $x \in (a, b)$ orthogonal to the driving direction. Suppose the center of the road is a straight line $x\mathbf{n}$, $x \in (a, b)$, $\mathbf{n} \in \mathbb{R}^2$. We define the projection $\mathcal{P}_x : \mathbb{R} \times L^1(\mathbb{R}^2, \mathbb{R}^+) \rightarrow \mathbb{R}$ as

$$\mathcal{P}_x(\xi) = \int_{-z/2}^{z/2} \xi(xn + yn^\perp) dy = \tilde{\xi}(x), \quad (3.1)$$

where z denotes the width of the road. In Figure 1 the averging is sketched for one edge.

In order to model the influence of the pedestrian flow on the road traffic, we extend the traffic flux function to

$$f(\rho, \tilde{\xi}) = \rho g_{PtoT}(\tilde{\xi}) V(\rho), \quad (3.2)$$

where the rate of driving g_{PtoT} is decreasing with increasing pedestrian density. If there are no people on the street the cars should behave as in the original model, i.e. g_{PtoT} is 1 for $\tilde{\xi} = 0$, whereas on a fully crowded road the cars should not drive at all, i.e. g_{PtoT} is 0 for $\tilde{\xi} = \xi_m$. One possible choice is

$$g_{PtoT}(\tilde{\xi}) = (1 - \tilde{\xi}/\xi_m)^{n_1}, \quad n_1 \geq 1. \quad (3.3)$$

The exponent n_1 depends on the situation we want to consider. In front of a school for example we should use n_1 large to enforce a stronger reduction of speed.

3.2. Traffic to pedestrian

From the perspective of the pedestrians the cars on the road occupy some space in their 2D region. To reflect this we extend the 1D traffic data onto the domain of the pedestrians.

Prolongation: Suppose that the road is located at $x\mathbf{n}, x \in (a, b), \mathbf{n} \in \mathbb{R}^2$. We define the characteristic function for the road i as

$$\begin{aligned} \chi_i &= \chi_0((\mathbf{x} - \mathbf{nx}) \cdot \mathbf{n}) \cdot \chi_{(-z/2, z/2)}((\mathbf{x} - \mathbf{nx}) \cdot \mathbf{n}^\perp) \\ &+ \chi_{(-z/2, 0)}((\mathbf{x} - a) \cdot \mathbf{n}) \cdot \chi_{(-z/2, z/2)}((\mathbf{x} - \mathbf{nx}) \cdot \mathbf{n}^\perp) \\ &+ \chi_{(0, z/2)}((\mathbf{x} - b) \cdot \mathbf{n}) \cdot \chi_{(-z/2, z/2)}((\mathbf{x} - \mathbf{nx}) \cdot \mathbf{n}^\perp). \end{aligned}$$

The road is not only stretched to the width z , but also elongated at both ends. This construction is chosen in order to avoid empty edges when two or more roads overlap, as illustrated in Figure 2. Based on this we define the 2D car density of the road i as

$$\begin{aligned} \tilde{\rho}_i(\mathbf{x}) &= \rho_i(x) (\chi_0((\mathbf{x} - \mathbf{nx}) \cdot \mathbf{n}) \cdot \chi_{(-z/2, z/2)}((\mathbf{x} - \mathbf{nx}) \cdot \mathbf{n}^\perp)) \\ &+ \bar{\rho}_i(a) (\chi_{(-z/2, 0)}((\mathbf{x} - a) \cdot \mathbf{n}) \cdot \chi_{(-z/2, z/2)}((\mathbf{x} - \mathbf{nx}) \cdot \mathbf{n}^\perp)) \\ &+ \bar{\rho}_i(b) (\chi_{(0, z/2)}((\mathbf{x} - b) \cdot \mathbf{n}) \cdot \chi_{(-z/2, z/2)}((\mathbf{x} - \mathbf{nx}) \cdot \mathbf{n}^\perp)). \end{aligned} \quad (3.4)$$

As data for the extensions at the ends we can use the respective junction values $\bar{\rho}$. The averaged 2D car density $\tilde{\rho}$ of a network of M roads is thus given by

$$\tilde{\rho}(\mathbf{x}) = \begin{cases} \frac{\sum_i^M \tilde{\rho}_i(\mathbf{x})}{\sum_i^M \chi_i} & , \text{ if } \sum_i^M \chi_i(\mathbf{x}) > 0 \\ 0 & , \text{ else.} \end{cases} \quad (3.5)$$

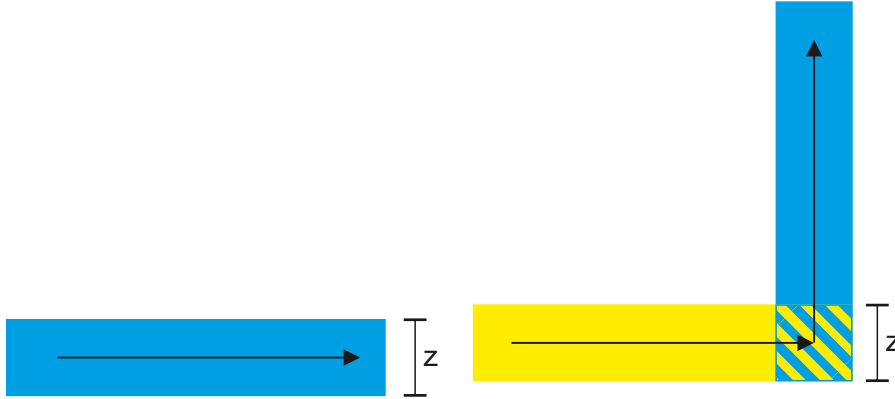


Fig. 1: Enlarged road.

Fig. 2: Enlarging the roads and filling the corners.

The influence of the vehicular traffic on the speed of the pedestrians we model by modifying (2.6) to

$$U(\xi, \tilde{\rho}) = g_{TtoP}(\tilde{\rho})U(\xi). \quad (3.6)$$

Accordingly the flux function (2.5) is changed to

$$\mathbf{F}(\xi, \tilde{\rho}) = \xi U(\xi, \tilde{\rho}) \mathbf{Z} . \quad (3.7)$$

For the pedestrian crossing rate $g_{TtoP} \in [0, 1]$ different choices might be reasonable. The first one is similar to (3.3)

$$g_{TtoP}^{(1)}(\tilde{\rho}) = (1 - \tilde{\rho}/\rho_m)^{n_2} , \quad (3.8)$$

i.e. the more cars are on the road, the more careful the pedestrians have to cross the street. Again, the exponent n_2 depends on the situation. Another possibility is to relate the hindrance of the pedestrians to the speed of the cars. This leads to a coupling of the form

$$g_{TtoP}^{(2)}(\tilde{\rho}) = (\tilde{\rho}/\rho_m)^{n_2} , \quad (3.9)$$

i.e. the faster the cars move, the more complicated is the passage for the pedestrians. Finally we introduce as third option the coupling function

$$g_{TtoP}^{(3)}(\tilde{\rho}) = \left(1 - \tilde{\rho}/\rho_m \left(1 - \frac{\tilde{\rho}}{\rho_m}\right)\right)^{n_2} . \quad (3.10)$$

Here the pedestrians prefer to cross the street, if there are few but very fast cars or there are many, but very slow cars. In all above coupling conditions the exponent n_2 can be used to model the sensitivity of the pedestrians. Higher exponents lead to more distinguished decisions of the pedestrians, whereas smaller values represent a less rigid judgement on the situations.

Remark 3.1. If the car traffic or the pedestrian flow is described by two equations for density $\tilde{\rho}$ and mean velocity \tilde{u} , as e.g. in the AW-Rascle equations [3], then more sophisticated coupling conditions could be applied. For example, conditions like

$$g_{TtoP}(\tilde{\rho}) = (1 - \tilde{\rho}/\rho_m)(1 - \tilde{u}/u_m)$$

seem to be more appropriate for the complex decision-making process of the pedestrians.

4. Numerical methods and results

In this section we study the behavior of the above discussed model numerically. Several test cases compare the influence of the choice of the coupling conditions.

For the numerical methods we discretize the roads into cells of a constant width h and the 2D domain of the pedestrians with a quadratic grid of the same spacing. The respectively averaged densities are denoted by ρ^i and ξ_{ij} .

4.1. Projections

In order to facilitate the discretization of the projections, we consider only roads aligned with the 2D grid of the pedestrians.

Pedestrian to Traffic: Consider a situation as depicted in Figure 3. The indices of the cells orthogonal to the orientation of the road are given by $\{\xi_{ij-s}, \dots, \xi_{ij}, \dots, \xi_{ij+s}\}$. Then formula (3.1) can be approximated by

$$\tilde{\xi}^i = \frac{1}{2s+1} \sum_{ij \in \{ij-s, \dots, ij+s\}} \xi_{ij}, \quad s = \left\lfloor \frac{z}{2h} \right\rfloor,$$

where z is the width of the road, h the grid spacing and $\lfloor \cdot \rfloor$ denotes the floor function.

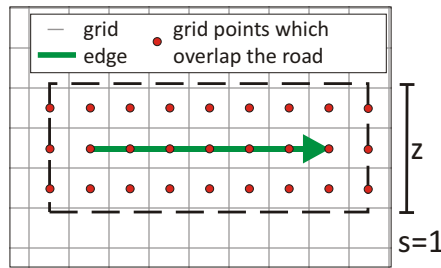


Fig. 3: Illustration of the restriction of the pedestrian data onto a 1D road.

Traffic to Pedestrian: Since the roads are discretized such that their grid is aligned with the grid of the pedestrians, we can easily evaluate the expression (3.5) for $\tilde{\rho}$. To every grid point $\mathbf{x}_{ij} \in \mathbb{R}$ in the pedestrian domain, we can find all points of the roads which contribute to the discrete prolonged car density $\tilde{\rho}_{ij}$. If there is no road closer than $z/2$ to \mathbf{x}_{ij} , $\tilde{\rho}_{ij}$ is set to 0. In case that only one road is nearby, we can just pick the value at the associated road section, as depicted in Figure 6. If several streets are involved or at a junction point, we simply average over all contributions as in (3.5). Here we recall, that due to formula (3.4), the junction values can appear in the $2D$ domain, although they have no spatial representation in the road network. This enlargement is introduced in order to avoid shorter passages for the pedestrians at junctions, as shown in Figure 4.

4.2. Numerical methods

For the solution of the 1D conservation law on the network we use a classical Godunov scheme. The 2D conservation law for pedestrians is solved using the FORCE scheme, see [38]. The eikonal equation is solved by a fast marching method and implemented as discussed in [36]. We solve the coupled problem by a first order splitting method:

Algorithm (Coupling procedure)

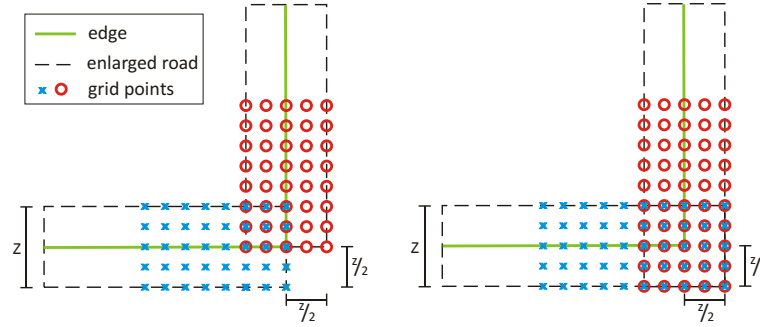


Fig. 4: Enlarging the roads and filling corners.

- (1) Project the pedestrian density onto the network as described in section 4.1.
- (2) Compute f at the cell interfaces.
- (3) Update the traffic network $t \rightarrow t + \Delta t$.
- (4) Project the new traffic density onto the pedestrian domain as described in section 4.1.
- (5) Compute the speeds $U(\xi, \tilde{\rho})$ according to (3.6).
- (6) Solve the eikonal equation (2.7) for the actual time step.
- (7) Compute the pedestrian fluxes at the cell interfaces by (3.7).
- (8) Update the pedestrian densities $t \rightarrow t + \Delta t$.

4.3. Numerical convergence of the coupling procedure

In order to verify the numerical method we study the numerical convergence on the following test problem. Consider a single road from $v_1 = (0, 0.5)$ to $v_2 = (1, 0.5)$. The maximal density is $\rho_m = 1$ and the maximal velocity is $V_m = 1$. As initial condition for the cars we choose $\rho_{init}(x) = 0.5, \forall x$ and set the boundary condition to $\rho_{bound}(t) = 0.5, \forall t$. The road width is $z = 0.2$, the pedestrian domain $\Omega = [-0.1, 1.1] \times [-0.1, 1.1]$ and the pedestrian destination $\Omega_D = [0, 0.1] \times \{-0.1\}$ (bottom boundary of Ω). As initial condition for ξ we choose

$$\xi_0(x, y) = \begin{cases} 0.5, & \text{if } (x, y) \in [0.4, 0.8] \times [0.6, 1] \\ 0, & \text{else.} \end{cases}$$

The coupling functions are (3.8) and (3.3) with $n_1 = n_2 = 1$. The reference solution is computed with a grid spacing of $h = \frac{1}{240}$ and $\Delta t = \frac{1}{240}$. For coarser grids the time step grows linearly as h .

| h | $L_\infty \rho$ | \mathcal{O} | $L_\infty \xi$ | \mathcal{O} |
|-------|---------------------|---------------|----------------|---------------|
| 1/10 | 0.001 | | 0.010 | |
| 1/20 | $7.2 \cdot 10^{-4}$ | 1.3 | 0.0065 | 0.77 |
| 1/30 | $3.8 \cdot 10^{-4}$ | 1.5 | 0.0049 | 0.67 |
| 1/40 | $2.3 \cdot 10^{-4}$ | 1.6 | 0.0037 | 0.95 |
| 1/60 | $1.1 \cdot 10^{-4}$ | 1.8 | 0.0026 | 0.87 |
| 1/80 | $6.3 \cdot 10^{-5}$ | 1.9 | 0.0019 | 1.09 |
| 1/120 | $2.5 \cdot 10^{-5}$ | 2.2 | 0.0011 | 1.4 |

(a) Numerical convergence of the coupling model

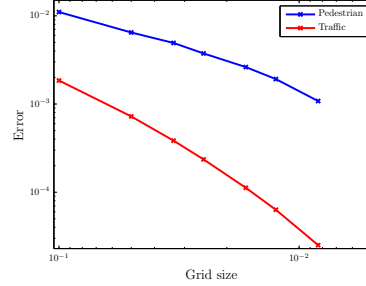
(b) $L_\infty \rho$ for different grid sizes h .

Fig. 5: Convergence of the numerical method

In Figure 5 the errors and the rates of convergence for different grid sizes at time $T = 1$ are shown. The numerical convergence is close to order 1 in case of the pedestrians and even better for the road traffic. The advantage of the car model, is that the Godunov method is less diffusive than the FORCE scheme and no extra equation as the eikonal equation has to be solved.

4.4. Comparison of coupling functions

In the following the influence of the choice of the coupling conditions on the overall dynamics of the model is investigated. Therefore we choose a specific test case and compare the results of different coupling functions g_{TtoP} .

We consider an example of two roads with different maximal velocities. The vertices of the network are located at

$$v_1 = (0, 2), v_2 = (1, 1), v_3 = (1, 2).$$

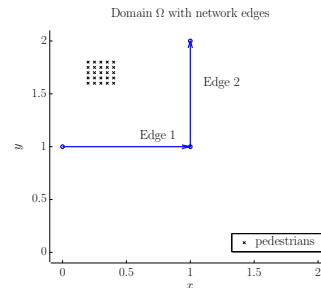


Fig. 6: Network plot with pedestrian initial condition.

The first edge $e_1 = (v_1, v_2)$ has maximal velocity $V_m = 2$ and $\rho_m = 1$, whereas the second edge $e_2 = (v_2, v_3)$ has $V_m = \rho_m = 1$. We choose the initial conditions

for the network as $\rho_{1,init}(x) = 0.5 - \sqrt{0.125}$, $\rho_{2,init}(x) = 0.5 \forall x$ and the boundary condition as $\rho_{1,bound}(t) = 0.5 - \sqrt{0.125}$, $\forall t$. For the pedestrian domain we set $\Omega = [-0.1 \ 2.1] \times [-0.1 \ 2.1]$ and choose a road width of $z = 0.2$. The destination of the pedestrians is $\Omega_D = [-0.1 \ 2.1] \times \{-0.1\} \cup \{2.1\} \times [-0.1 \ 2.1]$ (bottom and right boundary of Ω). The pedestrian initial condition is

$$\xi_0(x, y) = \begin{cases} 0.5, & \text{if } (x, y) \in [0.2 \ 0.4] \times [1.6 \ 1.8] \\ 0, & \text{else.} \end{cases}$$

In the coupling conditions the exponents $n_1 = 4$ and $n_2 = 1$ are used and for the numerical computations the grid size is $h = 0.05$ and the time steps are $\Delta t = 0.025$.

We consider three test cases, one for each choice of $g_{TtoP}^{(i)}$ for $i = 1, 2, 3$. In Figures 7 to 10 one can see the resulting traffic density on the left and the pedestrian density on the right.

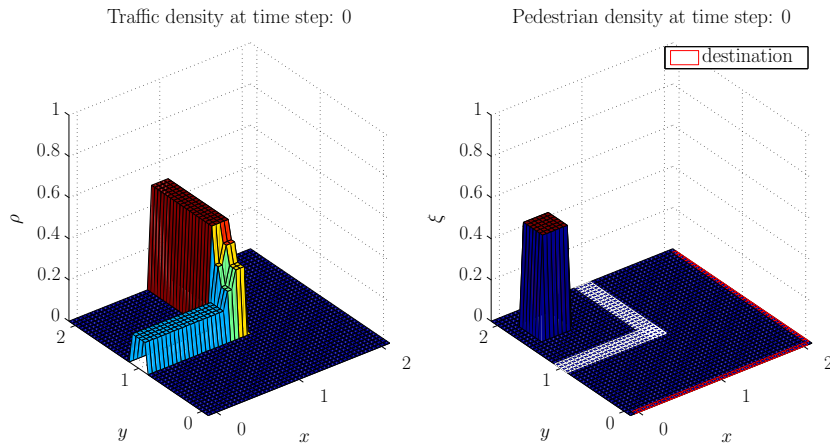


Fig. 7: Initial condition for all test cases.

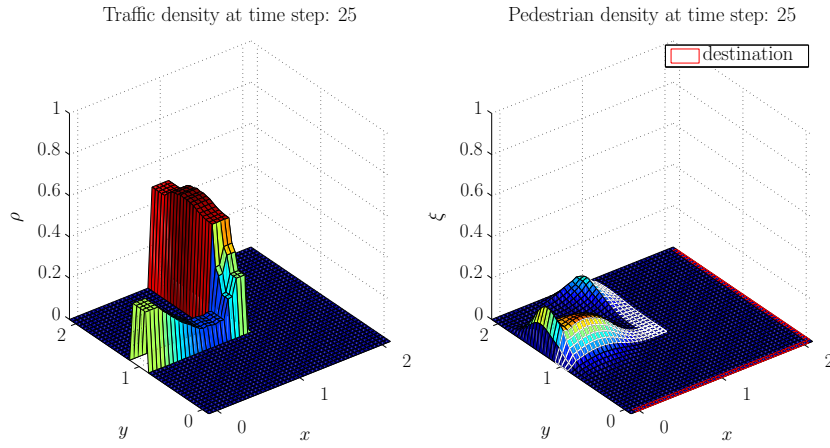


Fig. 8: Test case 1: Densities with coupling function $g_{TtoP}^{(1)}(\rho)$. Most of the pedestrians choose the first edge to cross the road.

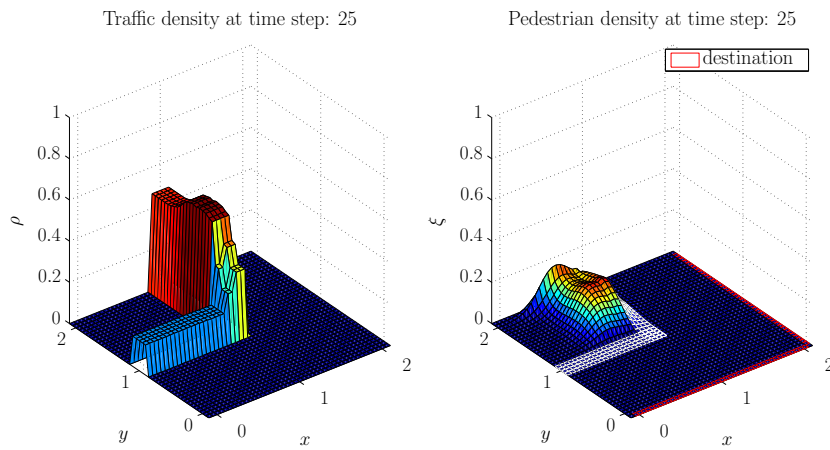


Fig. 9: Test case 2: Densities with coupling function $g_{TtoP}^{(2)}(\rho)$. Most of the pedestrians choose the second edge to cross the road.

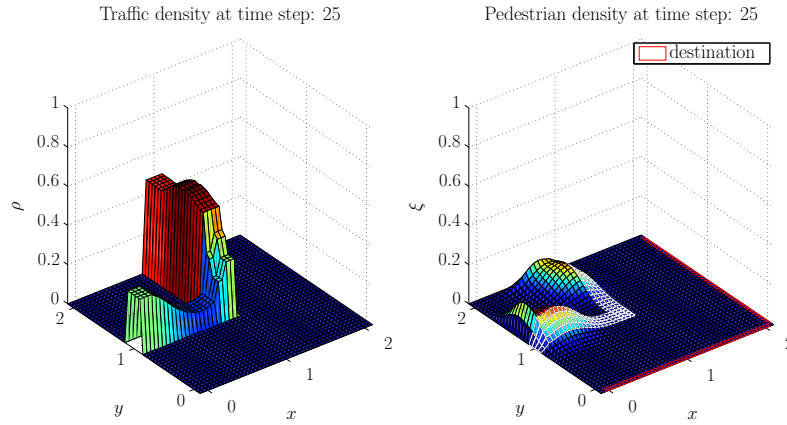


Fig. 10: Test case 3: Densities with coupling function $g_{TtoP}^{(3)}(\rho)$. One half of the pedestrians takes the first and the other half the second road.

The pedestrians are trapped in the upper left corner, so they need to cross one road. Which one depends strongly on the coupling conditions. In Figure 8 we observe that most of the pedestrians choose the road with the smaller density. In the second case, where the coupling condition depends on the velocity, most of the pedestrians choose the road with smaller maximal velocity but greater density (compare Figure 9). In Figure 10 it does not matter which road to take since the fluxes are the same. Thus the pedestrians split up into two groups of equal size, both choosing their shortest path to the destination.

The above examples show that the solution strongly depends on the choice of the coupling conditions. Therefore a careful selection of the appropriate functions is necessary in order to obtain realistic results.

4.5. Crosswalk

An interesting example to investigate the interaction of pedestrians and cars is a crosswalk. Therefore we consider two vertices

$v_1 = (0 \ 0.5)$, $v_2 = (1 \ 0.5)$,
 and connect them via one edge:
 $e_1 = (v_1, v_2)$.

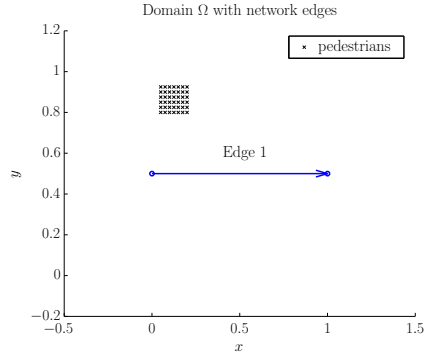


Fig. 11: Network for the crosswalk with pedestrian initial condition.

To model the priority of the pedestrians at the crosswalk on the edge, we choose at the location of the crosswalk a different exponent for the coupling function. For the coupling function on the edge we take $n_2 = 1$ on the crosswalk and $n_2 = 5$ otherwise. The maximal density and maximal velocity are $\rho_m = V_m = 1$. As the initial condition for the network we set $\rho_{init}(x) = 0.5 \forall x$ and the boundary condition to $\rho_{bound}(t) = 0.5, \forall t$. The grid size is $h = 0.025$, $\Delta t = 0.025$ and the road width is $z = 0.1$. For the pedestrian domain we choose $\Omega = [-0.05 \ 1.05] \times [-0.05 \ 1.05]$ and set the destination as $\Omega_D = [0.0 \ 0.3] \times \{-0.1\}$ (left-bottom boundary of Ω). The pedestrian initial condition is

$$\xi_0(x, y) = \begin{cases} 0.5, & \text{if } (x, y) \in [0.05 \ 0.2] \times [0.8 \ 0.95] \\ 0, & \text{else} \end{cases}$$

and coupling function g_{PtoT} is $g_{PtoT}(\xi) = (1 - \xi/\xi_m)^4$. For the domain of the crosswalk we set $\Omega_{cross} = [0.4 \ 0.6] \times [0.45 \ 0.55]$.

Now we investigate numerically whether the pedestrians choose the crosswalk (although this way to their destination is longer) or if they choose the shorter path where they are more hindered by cars. In the following Figures 12 to 16 the traffic density on the left and the pedestrian density on the right are plotted. Initially the roads have the same initial density and the pedestrians are located in the upper left corner, Figure 12. Then the pedestrians walk towards the crosswalk and enter the road on it, Figure 13. Due to this crossing, congestion in front of the crosswalk arises, Figure 14. In time step 38 the first pedestrians reach the destination. In Figure 15 we can see a small congestion of pedestrians in front of the destination. This is due to the fact that at this point people from top and right want to leave the domain at the corner point of Ω_D . When all pedestrians have crossed the road, the congestion in traffic relaxes again towards the initial state, Figure 16.

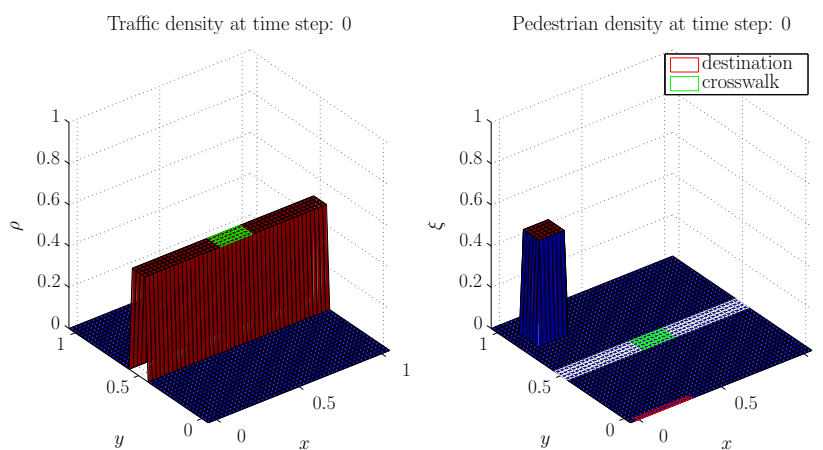


Fig. 12: Crosswalk at time step 0: Initial condition of the crosswalk.

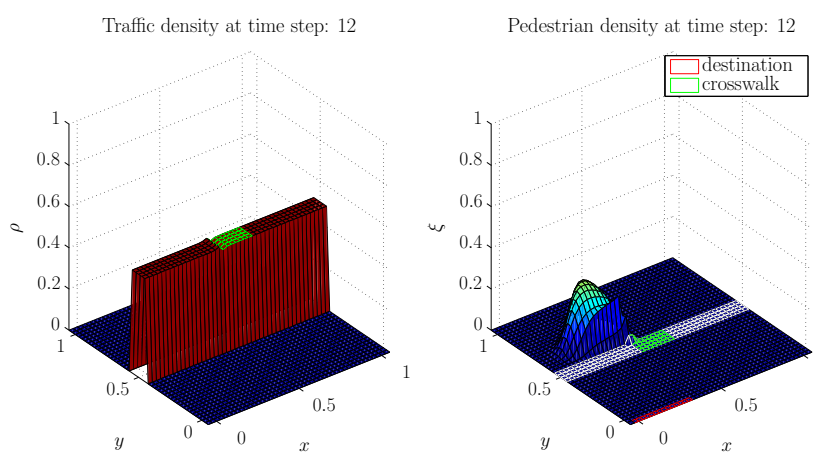


Fig. 13: Crosswalk at time step 12: Pedestrians enter the road on the crosswalk.

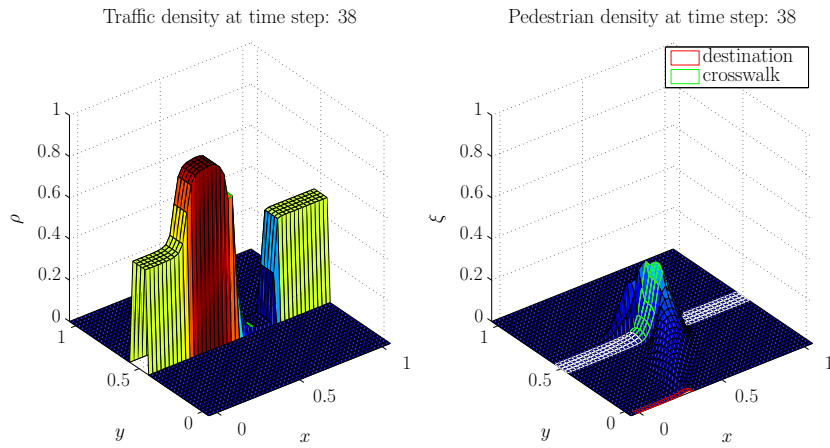


Fig. 14: Crosswalk at time step 38: A congestion arises in front of the crosswalk. The first pedestrians reach the destination.

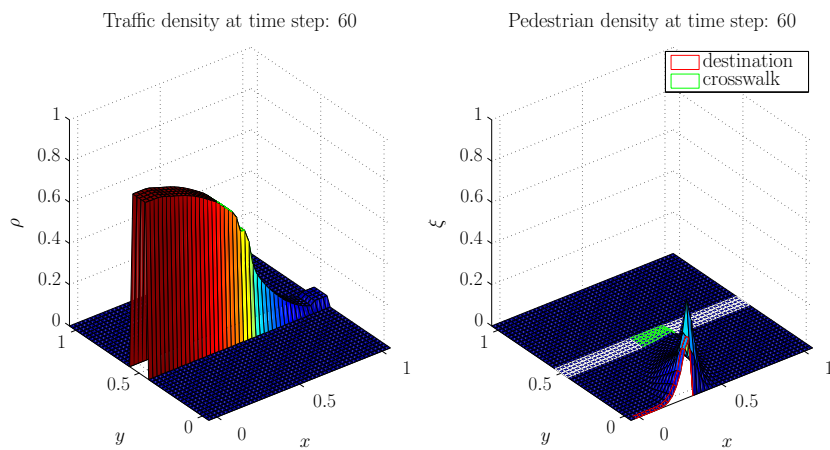


Fig. 15: Crosswalk at time step 60: The congestion has reached the front of road one and most of the pedestrians already have crossed the street.

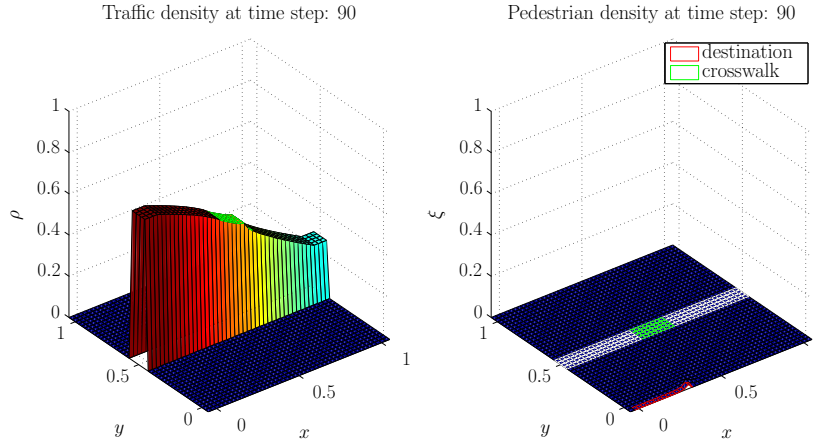


Fig. 16: Crosswalk at time step 90: All pedestrians have crossed the road and the congestion wave relaxes.

In conclusion, as one observes, with the above assumptions, pedestrians choose the crosswalk to cross the road even though this way is longer.

4.6. Rectangle

Finally, we consider a network which forms a rectangle with one ingoing and one outgoing road. The vertices are given by

$$\begin{aligned} v_1 &= (0, 1.5), v_2 = (1, 1.5), \\ v_3 &= (1, 2.5), v_4 = (1, 0.5), \\ v_5 &= (2, 2.5), v_6 = (2, 0.5), \\ v_7 &= (2, 1.5), v_8 = (3, 1.5) \end{aligned}$$

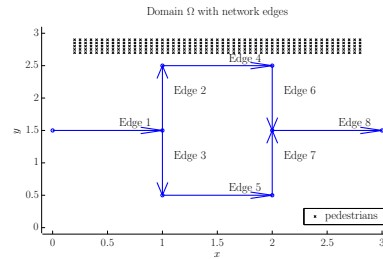


Fig. 17: Rectangle network with pedestrian initial condition.

and construct eight edges as shown in Figure 17. We use e_i for Edge i as short form. The maximal density and maximal velocity is given by $\rho_m = V_m = 1$ on every edge. As initial conditions for the network we set $\rho_{1,init}(x) = \rho_{8,init}(x) = 0.5 \forall x$ and $\rho_{i,init}(x) = 0.5 - \sqrt{0.125} \forall x$ and $i = 2, \dots, 7$. The external boundary condition for the network is $\rho_{1,bound}(t) = 0.5, \forall t$. As grid size we choose $h = 0.05, \Delta t = 0.05$ and

set the road width to $z = 0.2$. The pedestrian domain is $\Omega = [-0.1 \ 3.1] \times [-0.1 \ 3.1]$ with the destination $\Omega_D = [-0.05 \ 3.05] \times \{-0.1\}$ (bottom boundary of Ω). As initial condition for the pedestrians we set

$$\xi_0(x, y) = \begin{cases} 0.5, & \text{if } (x, y) \in [0.2 \ 0.8] \times [2.7 \ 2.9] \\ 0, & \text{else.} \end{cases}$$

The coupling functions are (3.8) with $n_2 = 3$ and (3.3) with $n_1 = 4$. In the beginning it is unclear which way the pedestrians choose. Either they need to cross the network only once but with high density on this road, or they cross the network twice, where the density on both roads is much smaller. In the following Figures 18 to 23 we can see the traffic density on the left and the pedestrian density on the right. At first the traffic is stationary and the pedestrians are located on top (compare Figure 18). In Figure 19 we can see that first pedestrians choose edge e_4 to cross. Hence, in front of this edge congestion in traffic arises and on edge e_6 the density decreases. In Figure 20 we can observe that most of the pedestrians try to enter the inner of the rectangle. So they want to cross twice. The congestion on edge e_4 gets higher and there are no cars anymore on edge e_6 . Then, most of the pedestrians have entered the inner of the rectangle. Due to the crossing of pedestrians on edge e_2 , e_4 and e_6 , density on edge e_8 is smaller than before. Therefore a few pedestrians choose edge e_8 to cross. The traffic congestion has reached edge e_1 (compare Figure 21). In time step 60, the part of edge e_8 where pedestrians cross the street is now at the end of edge eight, since the part with smaller density is moving with the cars. At $t = 60$ the first pedestrians reach the destination (see Figure 22). Then the pedestrians leave the road and the traffic congestion relaxes again (compare Figure 23).

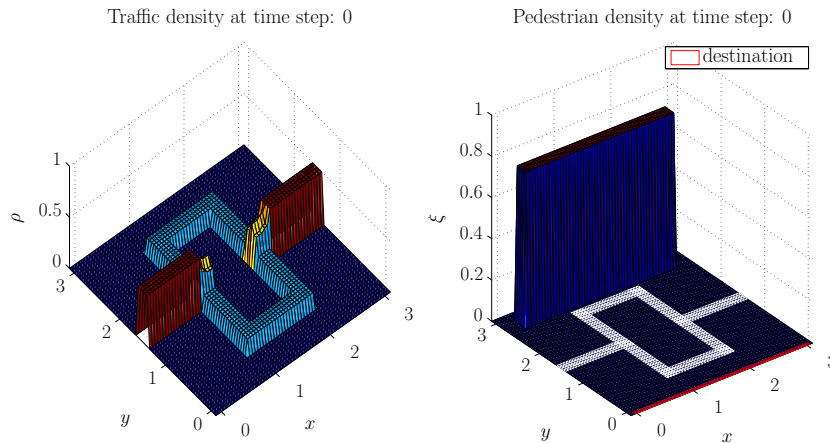


Fig. 18: Rectangle at time step 0: Initial condition of the rectangle.

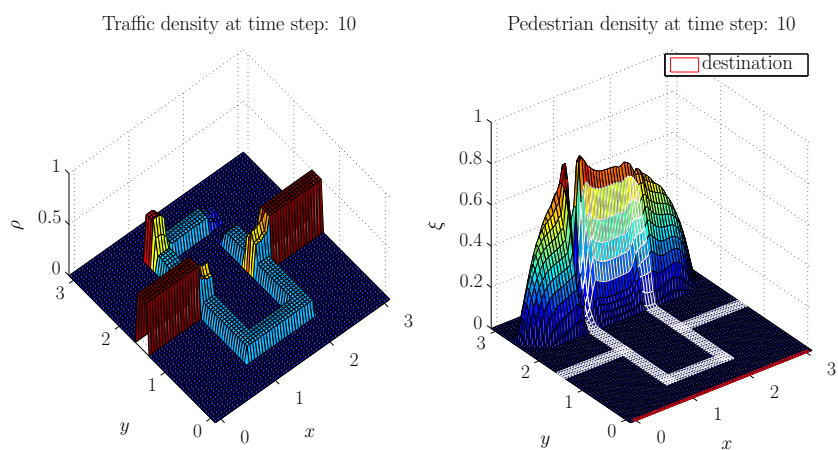


Fig. 19: Rectangle at time step 10: First pedestrians cross edge four.

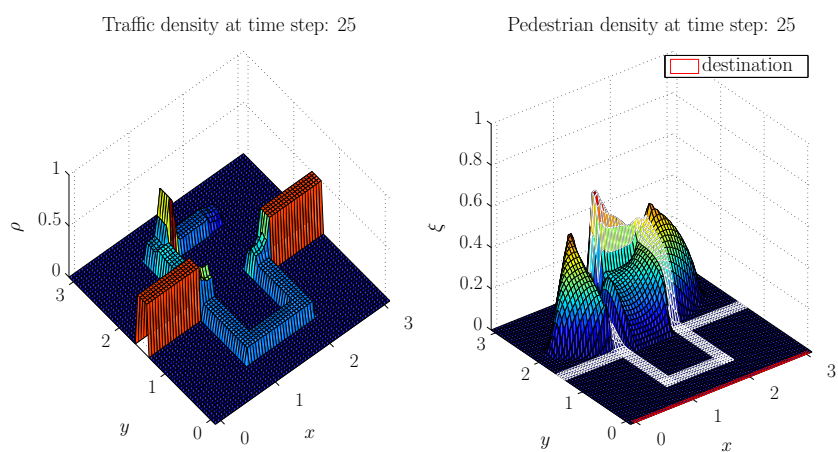


Fig. 20: Rectangle at time step 25: Most of the pedestrians try to enter the inner of the rectangle.

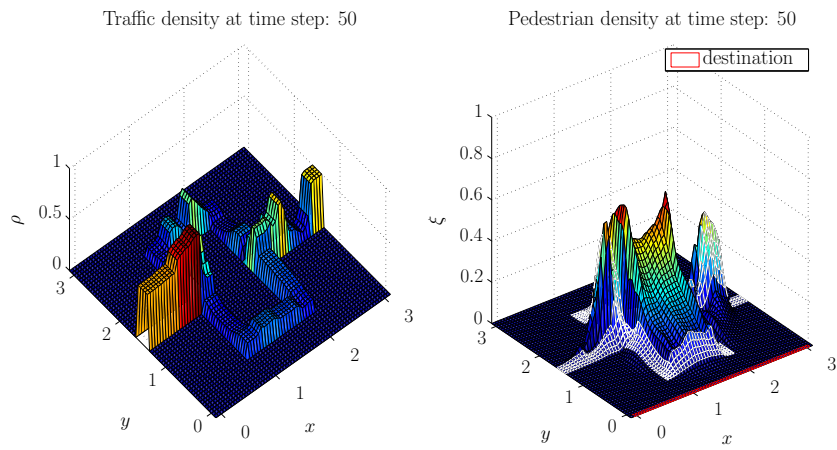


Fig. 21: Rectangle at time step 50: Most of the pedestrians have entered the inner of the rectangle. A few pedestrians choose edge e_8 to cross.

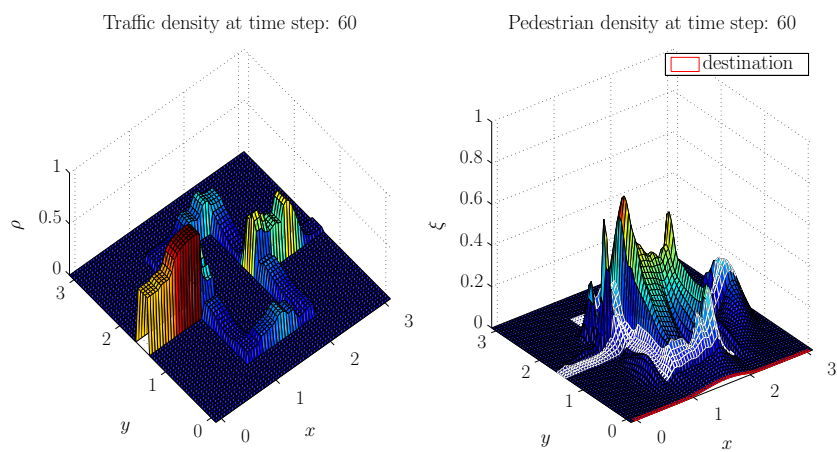


Fig. 22: Rectangle at time step 60: The part of edge eight where pedestrians cross the street is now at the end of edge eight.

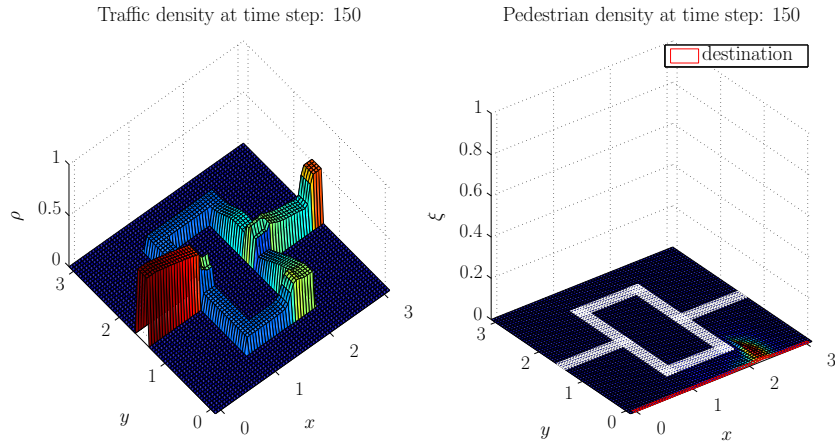


Fig. 23: Rectangle at time step 150: Most pedestrians reached the destination and the traffic congestion relaxes.

In conclusion, for these parameters most of the pedestrians choose the way where they have to cross the roads twice. Some pedestrians cross edge e_8 because the traffic density there was small enough due to crossings of pedestrians on other edges.

5. Concluding Remarks

We have developed a coupled model for pedestrian and traffic flow modeling the influence of the two flows on each other. The model is based on scalar macroscopic conservation laws and first order numerics. For the traffic flow we used the Lighthill-Whitham equation on networks and for the pedestrian dynamics Hughes' model. There we changed the flux functions by multiplying suitable coupling functions which may differ in special situations. To couple both systems we defined projections from $1D$ to $2D$ and vice versa. Then we have shown in different numerical experiments how the coupled model behaves and what influence the choice of coupling function has. Further research will include the development of higher order coupling and numerical procedures. Moreover, other traffic and pedestrian flow models can be coupled and more detailed coupled models can be developed.

References

1. D. Amadoria, M. Di Francesco, *The one-dimensional Hughes model for pedestrian flow: Riemann-type solutions*. Acta Mathematica Scientia, 32, 1, 2012, pp. 259-280
2. A. Aw, A. Klar, T. Materne, and M. Rascle, *Derivation of Continuum Traffic Flow Models from Microscopic Follow-the-Leader Models*. SIAM J. Appl. Math. 63 (1) (2002), pp. 259-278.
3. A. Aw and M. Rascle, *Resurrection of second order models of traffic flow*. SIAM J. Appl. Math., 60 (2000), pp. 916-938.

4. N. Bellomo, A. Bellouquid, *On the modelling of vehicular traffic and crowds by kinetic theory of active particles*, Model. Simul. Sci. Eng. Technol., (2010), pp. 273–296.
5. N. Bellomo, C. Dogbe, *On the Modeling of Traffic and Crowds: A Survey of Models, Speculations, and Perspectives*. Siam Review 53/3, (2011), pp. 409-463
6. N. Bellomo, C. Dogbe. *On the modelling crowd dynamics from scaling to hyperbolic macroscopic models*. Math. Models Methods Appl. Sci., 18 (Suppl.) (2008), pp. 1317-1345.
7. M. Bando, K. Hasebe, A. Nakayama, A. Shibata, and Y. Sugiyama, *Dynamical model of traffic congestion and numerical simulation*. Phys. Rev. E, 51 (1995), pp. 1035-1042
8. R. Bürger, K. Karlsen, J. Towers. *A conservation law with discontinuous flux modelling traffic flow with abruptly changing road surface conditions*, in: *Hyperbolic Problems: Theory, Numerics and Applications*. Proc. Sympos. Appl. Math., vol. 67, 2009, pp. 455-464.
9. G. M. Coclite and M. Garavello and B. Piccoli, *Traffic Flow on a Road Network*. SIAM J. Math. Anal., 3, 2005, 1862–1886
10. R. Colombo, M. Garavello, M. Lecureux-Mercier, *A Class of Non-Local Models for Pedestrian Traffic*. MMMAS 22 (4), 1150023, 2012
11. R. Colombo, M. Garavello, M. Lecureux-Mercier, *Non-local crowd dynamics*. Comptes Rendus Mathématique, 349 (13-14), 769-772, 2011
12. R. M. Colombo, M. D. Rosini, *Pedestrian flows and non-classical shocks*. Math. Methods Appl. Sci. 28 (13) (2005), pp. 1553-1567.
13. F. Berthelin, P. Degond, M. Delitla, M. Rascle, *A model for the formation and evolution of traffic jams*. Arch. Rat. Mech. Anal. 187, 185-220, 2008
14. C. Dogbe, *On the modelling of crowd dynamics by generalized kinetic models*. J. Math. Anal. Appl. 387, 512-532, 2012
15. M. Di Francesco, P.A. Markowich, J.F. Pietschmann, M. T. Wolfram, *On the Hughes model for pedestrian flow: The one-dimensional case*. J. Differential Equations 250 (2011), pp. 1334-1362
16. P. Goatin, *The Aw-Rascle vehicular traffic flow model with phase transitions*, Math. Comput. Modelling, 44 (2006), pp. 287-303.
17. J. Greenberg, *Extension and amplification of the Aw-Rascle model*. SIAM J. Appl. Math., 62 (2001), pp. 729-745.
18. A. Fuegenschuh, S. Goettlich, M. Herty, A. Klar, A. Martin, *A discrete optimization approach to Large Scale Supply Networks based on Partial Differential Equations*. SIAM Scient. Computing 30, 3, 1490-1507 2008
19. D. Helbing, *Traffic and related self-driven many-particle systems*. Rev. Modern Phys. 73 (4) (2001), pp. 1067-1141.
20. D. Helbing, *A fluid dynamic model for the movement of pedestrians*. Complex Systems 6, 391-415, 1992.
21. D. Helbing and P. Molnar, *Social force model for pedestrian dynamics*. Phys. Rev. E, 51 (1995), pp. 4282-4286.
22. D. Helbing, I.J. Farkas, P. Molnar, T. Vicsek, *Simulation of pedestrian crowds in normal and evacuation situations*. in: M. Schreckenberg, S.D. Sharma (Eds.), *Pedestrian and Evacuation Dynamics*, Springer-Verlag, Berlin, 2002, pp. 21-58.
23. M. Herty, A. Klar, *Modeling, Simulation and Optimization of Traffic Flow Networks*. SIAM Sci. Comp. 25 (3), 1066-1087, 2003
24. S. P. Hoogendoorn and P. H. L. Bovy, *State-of-the-art of vehicular traffic flow modelling*. J. Syst. Control Engrg., 215 (2001), pp. 283-303.
25. H. Holden and N. Risebro, *A mathematical model of traffic flow on a network of unidirectional road*. SIAM J. Math. Anal., 4 (1995), pp. 999-1017.

26. J. Lebacque and M. Khoshyaran, *First order macroscopic traffic flow models for networks in the context of dynamic assignment* in Transportation Planning?State of the Art, M. Patriksson and K. A. P. M. Labbe, eds., Kluwer Academic Publishers, Norwell, MA, 2002.
27. R. L. Hughes, *A continuum theory for the flow of pedestrians*. Transp. Res. Part B: Methodological 36 (6) (2002), pp. 507-535.
28. R. L. Hughes, *The flow of human crowds*. Annu. Rev. Fluid Mech. 35 (2003), pp. 169-182.
29. A. Klar and R. Wegener, *Enskog-like kinetic models for vehicular traffic*, J. Stat. Phys., 87 (1997), pp. 91-114.
30. H. Ling, S.C. Wong, M. Zhang, C.-H. Shu, W.H.K. Lam, *Revisiting Hughes dynamic continuum model for pedestrian flow and the development of an efficient solution algorithm*. Transp. Res. Part B: Methodological 43 (1) (2009), pp. 127-141.
31. B. Maury, A. Roudneff-Chupin, F. Santambrogio. *A macroscopic crowd motion model of the gradient-flow type*. Mathematical Models and Methods in Applied Sciences Vol. 20, No. 10 (2010), pp. 1787-1821.
32. A. D. May, *Traffic Flow Fundamentals*. Prentice-Hall, Englewood Cliffs, NJ, 1990
33. P. Nelson, *A kinetic model of vehicular traffic and its associated bimodal equilibrium solutions*. Transport Theory and Statistical Physics, 24 (1995), pp. 383-408.
34. B. Piccoli, A. Tosin, *Pedestrian flows in bounded domains with obstacles*. Contin. Mech. Thermodyn. 21 (2) (2009) 85-107.
35. I. Prigogine and R. Herman, *Kinetic Theory of Vehicular Traffic*. American Elsevier Publishing Co., New York, 1971.
36. J. A. Sethian, *Fast Marching Methods*. SIAM Review, 41, 1999, 199-235
37. G. Whitham, *Linear and Nonlinear Waves*. Wiley, New York, 1974.
38. E.F., Toro, *Riemann solvers and numerical methods for fluid dynamics*. Springer 2009
39. A. Treuille, S. Cooper, Z. Popovic, *Continuum crowds*. in: ACM Transaction on Graphics, Proceedings of SCM SIGGRAPH 2006, vol. 25, pp. 1160 - 1168.
40. M. Zhang, *A non-equilibrium traffic flow model devoid of gas-like behavior*. Transp. Res. B, 36 (2002), pp. 275-290